Molecular Cell, Vol. 16, 387–397, November 5, 2004, Copyright ©2004 by Cell Press

Phosphorylation of Cdc20 by Bub1 Provides a Catalytic Mechanism for APC/C Inhibition by the Spindle Checkpoint

Zhanyun Tang,[1] Hongjun Shu,[1] Dilhan Oncel, She Chen, and Hongtao Yu*
Department of Pharmacology
The University of Texas Southwestern Medical Center at Dallas
5323 Harry Hines Boulevard
Dallas, Texas 75390

Summary

To ensure the fidelity of chromosome segregation, the spindle checkpoint blocks the ubiquitin ligase activity of APC/C^{Cdc20} in response to a single chromatid not properly attached to the mitotic spindle. Here we show that HeLa cells depleted for Bub1 by RNA interference are defective in checkpoint signaling. Bub1 directly phosphorylates Cdc20 in vitro and inhibits the ubiquitin ligase activity of APC/C^{Cdc20} catalytically. A Cdc20 mutant with all six Bub1 phosphorylation sites removed is refractory to Bub1-mediated phosphorylation and inhibition in vitro. Upon checkpoint activation, Bub1 itself is hyperphosphorylated and its kinase activity toward Cdc20 is stimulated. Ectopic expression of the nonphosphorylatable Cdc20 mutant allows HeLa cells to escape from mitosis in the presence of spindle damage. Therefore, Bub1-mediated phosphorylation of Cdc20 is required for proper checkpoint signaling. We speculate that inhibition of APC/C^{Cdc20} by Bub1 in a catalytic fashion may partly account for the exquisite sensitivity of the spindle checkpoint.

Introduction

The genetic stability of an organism depends on the accurate segregation of chromosomes during cell division (Nasmyth et al., 2000; Nasmyth, 2002). Cells employ a multistep cascade to initiate chromosome segregation during mitosis (Nasmyth et al., 2000; Nasmyth, 2002). When all sister chromatids have been captured by the mitotic spindle and aligned at the metaphase plate, the anaphase-promoting complex or cyclosome (APC/C) ubiquitinates securin (Nasmyth et al., 2000; Harper et al., 2002; Nasmyth, 2002; Peters, 2002). Degradation of the ubiquitinated securin by the proteosome leads to the activation of separase, which then cleaves Scc1, a subunit of the cohesin protein complex (Nasmyth et al., 2000; Nasmyth, 2002). Loss of cohesion allows the two sets of chromatids to be evenly distributed to opposite poles via their attachment to spindle microtubules.

The spindle checkpoint ensures the fidelity of chromosome segregation by blocking the activity of APC/C in response to the existence of a single unattached or tension-lacking kinetochore (Nicklas, 1997; Shah and Cleveland, 2000; Musacchio and Hardwick, 2002; Yu, 2002). The molecular players of this checkpoint include Mad1, Mad2, Mad3, Bub1, Bub2, Bub3, and Mps1 (Musacchio and Hardwick, 2002; Yu, 2002; Bharadwaj and Yu, 2004). Both Mad2 and BubR1 can independently bind to Cdc20 and inhibit the activity of APC/C^{Cdc20}, a critical target of the spindle checkpoint (Fang et al., 1998a, 1998b; Tang et al., 2001; Fang, 2002). Inhibition of APC/C in vivo may involve the transient formation of a mitotic checkpoint complex (MCC) containing BubR1, Bub3, Mad2, and Cdc20 (Sudakin et al., 2001; Chen, 2002; Yu, 2002). There are conflicting reports with respect to the timing and mechanism of the formation of the MCC (Sudakin et al., 2001; Tang et al., 2001; Chen, 2002; Fang, 2002; Yu, 2002). According to one model, the unattached kinetochores serve as catalytic sites for the formation of the checkpoint complexes containing Mad2 and Cdc20 (Yu, 2002). These checkpoint complexes may then diffuse away from the kinetochores to inhibit APC/C throughout the cell. This view is consistent with recent structural studies on Mad1, Mad2, and Cdc20, which suggest that Mad2 may be passed on to Cdc20 from Mad1 at the unattached kinetochores (Luo et al., 2000, 2002, 2004; Sironi et al., 2002).

Less is known about the biochemical functions of Bub1 in checkpoint signaling. Human Bub1 phosphorylates Mad1 in vitro (Seeley et al., 1999). In yeast, the Bub1-Bub3 complex interacts with Mad1 when the spindle checkpoint is activated (Brady and Hardwick, 2000). Overexpression of a dominant allele of Bub1 in yeast causes a mitotic delay without spindle damage that is dependent on the functions of Bub2, Bub3, and Mad1-3 (Farr and Hoyt, 1998). These data suggest that Bub1 might regulate the function of Mad1 and act upstream of most checkpoint genes.

Here we report a rather surprising and direct role of Bub1 in checkpoint-dependent inhibition of APC/C. Bub1 directly phosphorylates Cdc20 and blocks the activity of APC/C^{Cdc20} in vitro. In contrast to BubR1 and Mad2, Bub1 inhibits APC/C^{Cdc20} in a catalytic fashion with its kinase activity required for this inhibition. The kinase activity of Bub1 toward Cdc20 is stimulated by an active spindle checkpoint. As a single unattached kinetochore within a cell is sufficient to activate the spindle checkpoint, the checkpoint-stimulated catalytic inhibition of APC/C by Bub1 might be partially responsible for this remarkable sensitivity of the checkpoint.

Results

Bub1 Is Required for the Spindle Checkpoint in Living Cells

Using RNA interference (RNAi), we depleted Bub1 from HeLa cells and examined the phenotypes of these cells in the presence of spindle-damaging agents, such as nocodazole. The protein levels of Bub1 were significantly reduced in cells treated with two different siRNA oligonucleotides against Bub1 (Figure 1A). Both Bub1 siRNAs caused similar phenotypes, and only the data for Bub1 siRNAa were shown. While about 90% of control cells arrested in mitosis in the presence of nocoda-

*Correspondence: hongtao.yu@utsouthwestern.edu
[1]These authors contributed equally to this work.

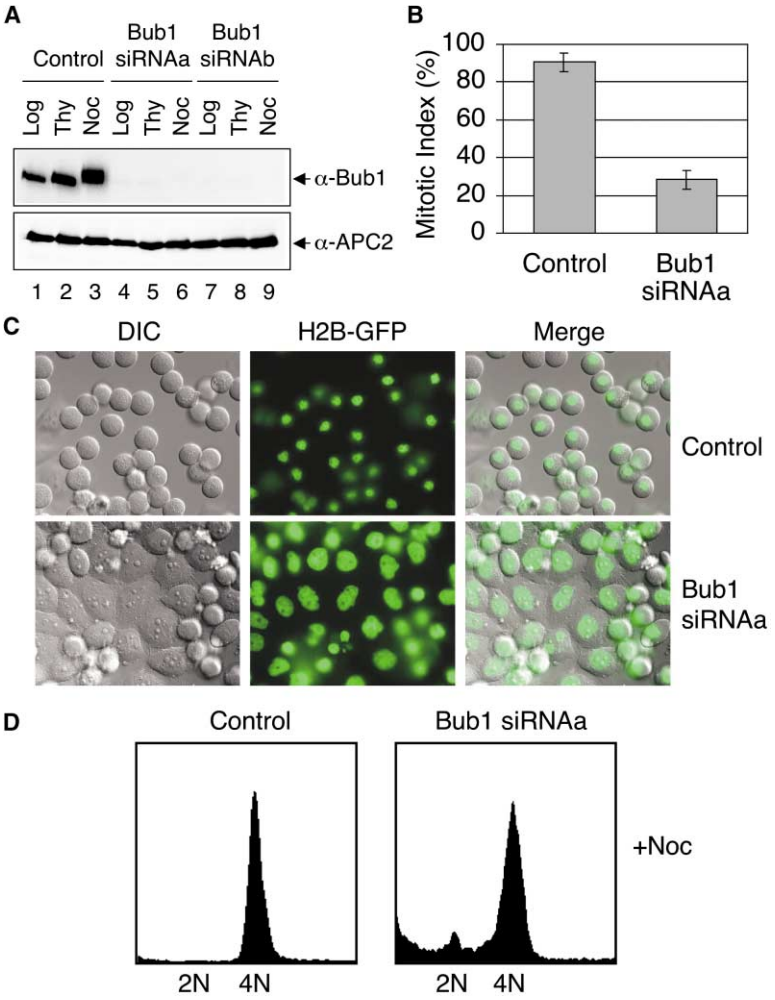

Figure 1. RNAi-Mediated Depletion of Bub1 Impairs the Spindle Checkpoint

(A) Log phase (Log), thymidine-arrested (Thy), or nocodazole (Noc)-arrested HeLa cells, which were transfected with control or Bub1 siRNAs, were dissolved in SDS sample buffer, separated on SDS-PAGE, and blotted with the indicated antibodies.

(B) HeLa-H2B-GFP cells were transfected for 36 hr with control or Bub1 siRNAa, treated with nocodazole (300 nM) for 16 hr, and directly visualized using an inverted fluorescence microscope. The mitotic index of these cells was measured by counting three fields of more than 100 cells.

(C) Representative fields of the cells described in (B). Both the cell and DNA morphologies are shown.

(D) FACS analysis of the cells described in (B). The 2N and 4N peaks are labeled.

zole, a significant fraction of HeLa cells depleted for Bub1 failed to undergo mitotic arrest (Figure 1B). These cells exited from mitosis without undergoing cytokinesis and possessed 4N DNA contents (Figures 1C and 1D). Thus, Bub1 is required for the mitotic arrest of HeLa cells in response to gross spindle damage.

Bub1 Phosphorylates Cdc20 In Vitro

Consistent with earlier findings (Taylor et al., 2001), the protein level of Bub1 dropped sharply as cells exited from mitosis, in keeping with its role in mitosis (Figures 2A and 2B). We next examined the interactions between Bub1 and other checkpoint proteins. Bub1 interacted with Bub3 in HeLa cells throughout the cell cycle (Figure 2C). Further fractionation of the cell lysates demonstrated that the majority of Bub1 was bound with Bub3 (data not shown). We did not observe significant interactions between Bub1 and other checkpoint proteins (data not shown).

Because Bub1 contains a protein kinase domain, we tested whether it phosphorylated proteins in the checkpoint pathway. Since Bub1 was always associated with Bub3 in HeLa cells, we coexpressed Bub1 or a kinase-inactive mutant of Bub1 (Bub1^{K821A}) together with Bub3 in Sf9 insect cells and purified the resulting Bub1-Bub3 and Bub1^{K821A}-Bub3 complexes (Figure 2D). Bub1-Bub3 phosphorylated recombinant Cdc20, while Bub1^{K821A}-Bub3 did not do so (Figure 2E). We also quantitated the amount of Cdc20 phosphorylated under these conditions. Assuming that each Cdc20 molecule was phosphorylated at one site on average, Bub1 phosphorylated 74% of Cdc20 in the kinase reaction at a Bub1:Cdc20 molar ratio of 1:10. Therefore, Bub1 phosphorylated a significant percentage of Cdc20 in these reactions. Recombinant Bub1 alone also efficiently phosphorylated Cdc20, indicating that Bub3 is not required for this process (data not shown).

We next tested a panel of kinases for their ability to phosphorylate Cdc20. Human polo-like kinase (Plk1), Mps1, Aurora A, Aurora B, BubR1, p38MAPK, and ERK1 failed to phosphorylate Cdc20 to a significant extent (Figure 2F). These kinases efficiently phosphorylated artificial substrates, such as MBP or casein (Figure 2F). Thus, phosphorylation of Cdc20 by Bub1 appears to be specific. Cdc20 has recently been shown to be phosphorylated in *Xenopus* egg extracts (Chung and Chen, 2003). Addition of chemical inhibitors of the MAP kinase cascade into these extracts caused the dephosphorylation of Cdc20 at certain sites, suggesting that MAPK might be involved in Cdc20 phosphorylation. However,

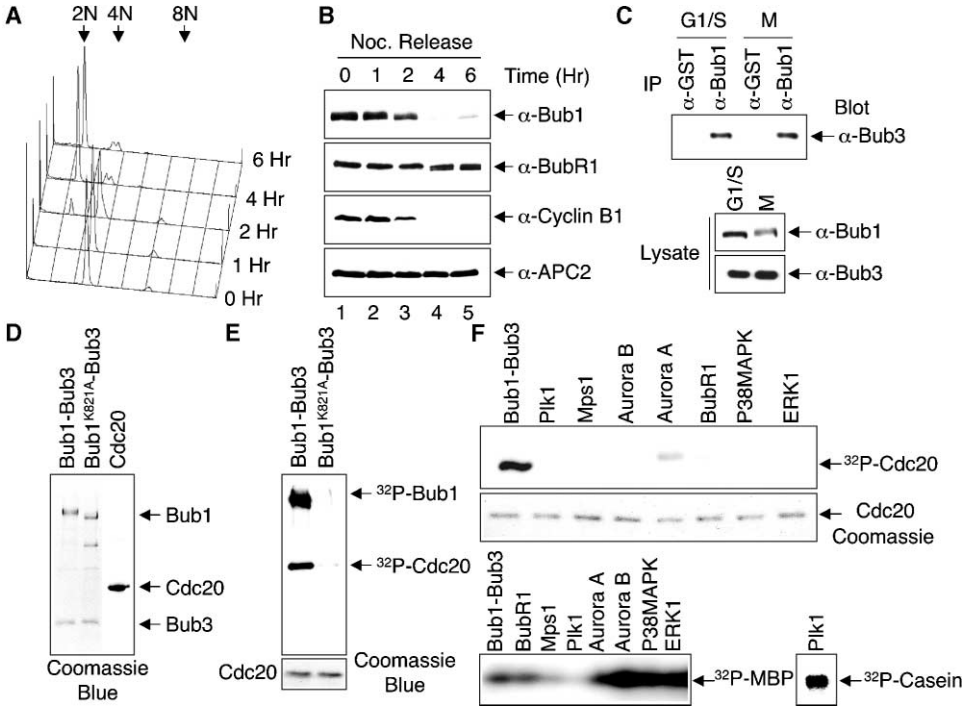

Figure 2. Bub1 Phosphorylates Cdc20 In Vitro

(A) FACS analysis of HeLa S3 cells treated with nocodazole for 18 hr and then released into fresh medium for the indicated time.

(B) The same HeLa S3 cells as in (A) were dissolved in SDS sample buffer, separated on SDS-PAGE, and blotted with the indicated antibodies.

(C) HeLa S3 cells were arrested at the G1/S boundary by thymidine or in mitosis by nocodazole, lysed, and immunoprecipitated with the indicated antibodies. Both the cell lysates and the immunoprecipitates were blotted with anti-Bub3.

(D) Recombinant purified Bub1-Bub3, Bub1^{K821A}-Bub3, and Cdc20 proteins produced in Sf9 cells were separated on SDS-PAGE and stained with Coomassie blue. The bands corresponding to Bub1, Bub3, and Cdc20 are labeled.

(E) Recombinant Bub1-Bub3 and Bub1^{K821A}-Bub3 proteins were incubated with Cdc20 in the presence of γ-^{32}P-ATP for 30 min at room temperature. The reaction mixture was quenched with SDS sample buffer, separated on SDS-PAGE, and analyzed by autoradiography. The positions of phosphorylated Cdc20 and Bub1 (presumably through autophosphorylation) are indicated. The bottom panel shows a Coomassie-stained gel of the same reactions to indicate that equal amounts of Cdc20 were included in these reactions.

(F) Several mitotic kinases were incubated with recombinant His$_6$-tagged Cdc20, MBP, or casein in the presence of γ-^{32}P-ATP for 30 min at room temperature. The middle panel shows a Coomassie-stained gel of the same reactions to indicate that equal amounts of Cdc20 were included in these reactions.

two members of the MAPK family, p38 and ERK1, failed to phosphorylate human Cdc20 in our in vitro kinase assays. We do not know the reason for this discrepancy. This might reflect a difference between the human and *Xenopus* Cdc20 proteins. Alternatively, MAPK might indirectly regulate Cdc20 phosphorylation in *Xenopus* extracts.

Bub1 Inhibits APC/C^{Cdc20} Catalytically In Vitro

We then tested the effects of Cdc20 phosphorylation by Bub1 on the activity of APC/C^{Cdc20} in a reconstituted APC/C ubiquitination assay using a fragment of human cyclin B1 (residues 1–102) as the substrate. Bub1-Bub3 greatly reduced the ubiquitin ligase activity of APC/C^{Cdc20} (Figure 3A). The highest Bub1:Cdc20 molar ratio used in the reactions was 1:10 (Figure 3A, lane 3). Thus, Bub1-Bub3 inhibited APC/C^{Cdc20} at substoichiometric amounts, suggesting that Bub1-Bub3 inhibited APC/C^{Cdc20} in a catalytic fashion. This was confirmed by the fact that Bub1^{K821A}-Bub3 failed to inhibit APC/C^{Cdc20}, indicating that inhibition of APC/C^{Cdc20} by Bub1-Bub3 required the kinase activity of Bub1 (Figure 3B). Inhibition of APC/C was more efficient when Cdc20 was preincubated with Bub1-Bub3, consistent with the notion that Cdc20, not APC/C itself, is the target of Bub1 in the in vitro ubiquitination assays (data not shown). Finally, Bub1-Bub3 did not substantially inhibit APC/C^{Cdh1} (Figure 3C). Taken together, these data indicate that Bub1-Bub3 inhibits APC/C^{Cdc20} catalytically by phosphorylating Cdc20.

Phosphorylation of Cdc20 by Bub1 required the intact Bub1 protein. Though capable of autophosphorylation, a C-terminal fragment of Bub1 (Bub1C) containing its kinase domain failed to phosphorylate Cdc20 (Figure 3E). Consequently, Bub1C failed to inhibit APC/C^{Cdc20} (Figure 3F). A Bub1 fragment lacking the kinase domain did not inhibit APC/C^{Cdc20} (Figure 3F), again indicating that the Bub1 kinase activity is required for its inhibition of APC/C^{Cdc20}.

Six Serine/Threonine Residues of Cdc20 Are Phosphorylated In Vivo and by Bub1 In Vitro

Using mass spectrometry, we mapped the in vivo phosphorylation sites of Cdc20 and the residues of Cdc20 phosphorylated by Bub1 in vitro. The endogenous Cdc20 protein isolated from nocodazole-arrested HeLa cells exhibited retarded gel mobility as compared to

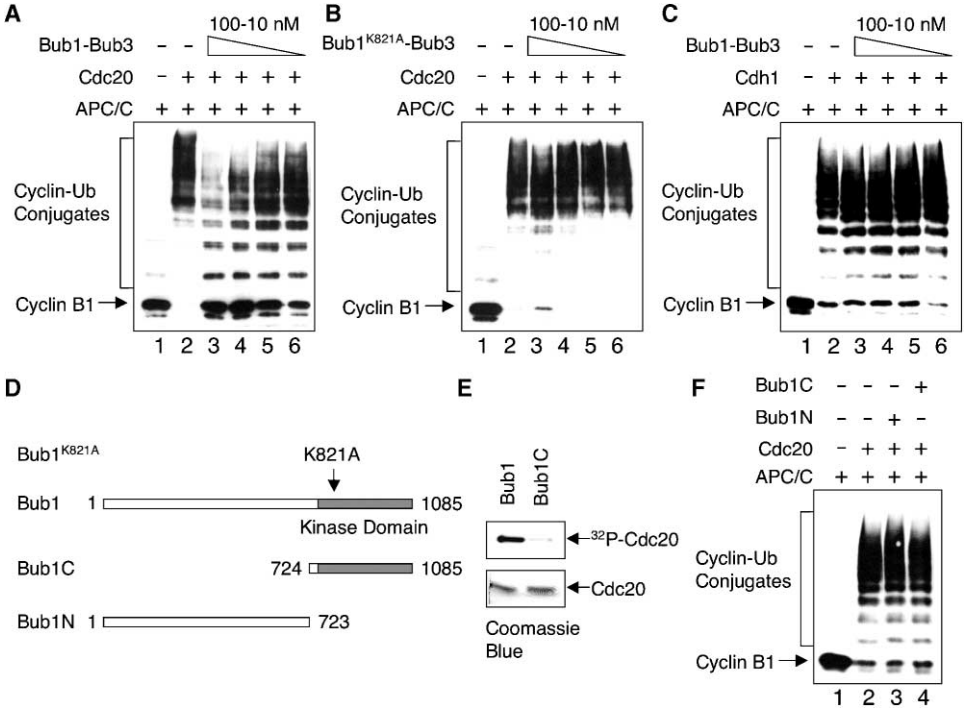

Figure 3. Bub1 Inhibits the Activity of APC/C^{Cdc20} Catalytically

(A) APC/C was isolated from interphase *Xenopus* egg extracts and incubated with recombinant human Cdc20 protein, in the presence of buffer (lane 2) and increasing amounts of Bub1 (lanes 3–6) with the addition of ATP. The ubiquitination activity of APC/C was assayed with a Myc-tagged N-terminal fragment (residues 1–102) of human cyclin B1. The reaction mixtures were separated on SDS-PAGE and blotted with the anti-Myc antibody. The positions of the cyclin B1 substrate and the cyclin B1-ubiquitin conjugates are labeled.

(B) Same as (A) except that the kinase-inactive Bub1^{K821A}-Bub3 protein was used instead of the wild-type Bub1-Bub3.

(C) Same as (A) except that the recombinant Cdh1 protein was used instead of Cdc20.

(D) Schematic drawing of the Bub1 fragments and mutants.

(E) Recombinant Bub1 and Bub1C proteins were incubated with Cdc20 in the presence of γ-^{32}P-ATP for 30 min at room temperature. The reaction mixture was quenched with SDS sample buffer, separated on SDS-PAGE, and analyzed by autoradiography. The position of phosphorylated Cdc20 is indicated. The bottom panel shows a Coomassie-stained gel of the same reactions to indicate that equal amounts of Cdc20 were included in these reactions.

(F) Same as (A) except that Bub1N (200 nM) and Bub1C (200 nM) proteins were used instead of the wild-type Bub1-Bub3.

Cdc20 from thymidine-arrested cells (Figures 4A and 4B). This mobility shift of Cdc20 was reversed with phosphatase treatment (Figure 4B), indicating that Cdc20 was phosphorylated in checkpoint-active cells. Recombinant Cdc20 protein was also efficiently phosphorylated by Bub1-Bub3 in vitro (Figure 4C). Either the endogenous Cdc20 protein from nocodazole-treated HeLa cells or the Cdc20 protein treated with Bub1-Bub3 was subjected to mass spectrometric analysis (Figure 4D). A total of six phosphorylation sites on the endogenous Cdc20 protein were identified (Figure 4E). All six sites were serine and threonine residues located in the N-terminal domain of Cdc20. Significantly, mass spectrometric analysis revealed that the same six serine/threonine residues of Cdc20 were phosphorylated by Bub1-Bub3 in vitro (Figure 4E). These results strongly suggest that Cdc20 is phosphorylated by Bub1 in vitro and in vivo. The phosphorylation sites on Cdc20 identified in this study differ from those identified by Kraft et al. (Kraft et al., 2003). This is possibly caused by the different ways of isolating Cdc20 in the two experiments. We purified the endogenous Cdc20 protein from nocodazole-arrested cells using an anti-Cdc20 antibody. Kraft et al. isolated Cdc20 using an anti-Cdc27 antibody. Only APC/C bound Cdc20 was expected to be immunoprecipitated by the anti-Cdc27 antibody. Therefore, we analyzed the phosphorylation patterns of the entire cellular population of Cdc20 while Kraft et al. only examined the APC/C bound pool of Cdc20.

To further confirm that Bub1 is required for Cdc20 phosphorylation in vivo, we next checked the phosphorylation status of Cdc20 in Bub1 RNAi cells. Because Bub1 RNAi cells did not undergo mitotic arrest efficiently in the presence of nocodazole, both control and Bub1 RNAi cells were first arrested at G1/S with thymidine and allowed to accumulate in mitosis in the presence of nocodazole after the removal of thymidine. The mitotic cells were shaken off the plates and lysed. The cell lysate was separated by SDS-PAGE and blotted with anti-Cdc27 and anti-Cdc20 antibodies. The cells were in mitosis, as indicated by the gel mobility shift of Cdc27 caused by phosphorylation (Figure 4F). Consistent with Bub1 playing a role in phosphorylating Cdc20 in vivo, the slower migrating and phosphorylated forms of

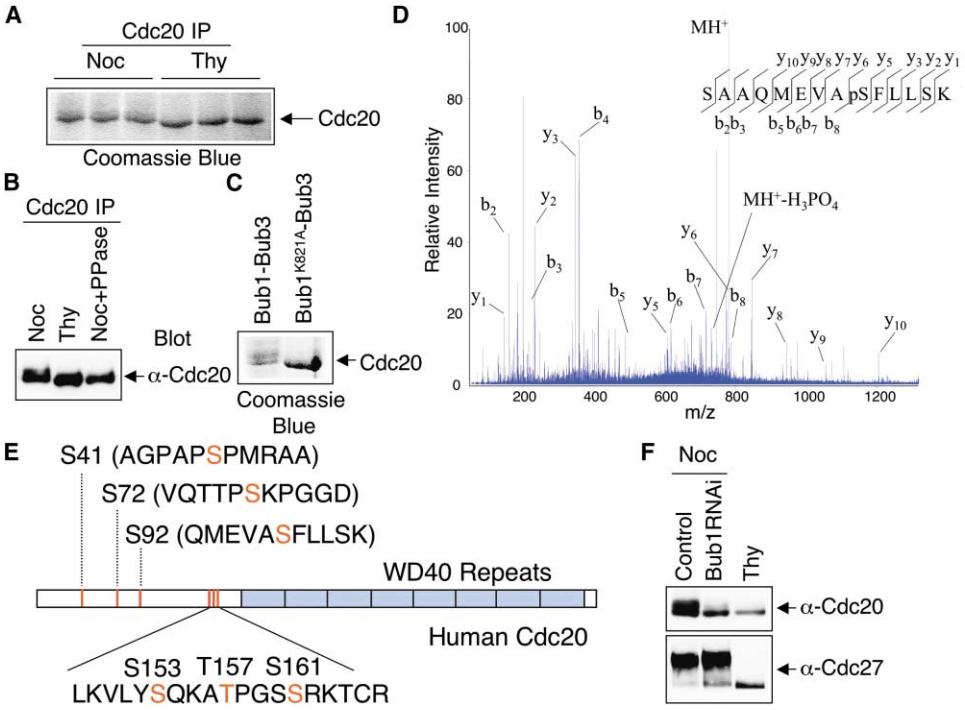

Figure 4. Mapping the In Vivo and In Vitro Phosphorylation Sites of Cdc20 by Mass Spectrometry

(A) The endogenous Cdc20 protein was immunoprecipitated from nocodazole- or thymidine-arrested cells, separated on SDS-PAGE, and stained with Coomassie.

(B) The same samples in (A) were blotted with anti-Cdc20 antibody. A fraction of the Cdc20 IP from nocodazole-arrested cells was also treated with λ-phosphatase.

(C) Purified recombinant Cdc20 protein was incubated with Bub1-Bub3 or Bub1^{K821A}-Bub3 in the presence of cold ATP for 2 hr at room temperature. The reactions mixtures were separated by SAS-PAGE and stained with Coomassie.

(D) Mass spectrometry spectrum showing the fragmentation pattern of a phosphopeptide identified in the endogenous Cdc20 protein.

(E) In vivo and in vitro Cdc20 phosphorylation sites identified by mass spectrometry.

(F) The cell lysates of control or Bub1 RNAi cells in mitosis were blotted with anti-Cdc20 and anti-Cdc27 antibodies. Cdc27 is a subunit of APC/C and is known to be phosphorylated in mitosis.

Cdc20 were absent in Bub1 RNAi cells (Figure 4F). Therefore, Bub1 is involved in the phosphorylation of Cdc20 in vivo.

Generation of a Cdc20 Mutant Refractory to Phosphorylation and Inhibition by Bub1

We mutated all six Bub1 phosphorylatable serine/threonine residues of Cdc20 to alanines. This Cdc20 mutant was named Cdc20^{BPM}, for *B*ub1 *p*hosphorylation site *m*utant. Recombinant Cdc20^{BPM} was only weakly phosphorylated by Bub1-Bub3 in vitro (Figure 5A), indicating that mutations of the six phosphorylation sites had eliminated most of Bub1-mediated phosphorylation of Cdc20. Importantly, Cdc20^{BPM} was as efficient as the wild-type Cdc20 protein (Cdc20^{WT}) in promoting the ubiquitin ligase activity of APC/C, and Bub1-Bub3 failed to inhibit the activity of the APC/C-Cdc20^{BPM} complex (Figure 5B). These results indicate that phosphorylation of Cdc20 by Bub1, rather than phosphorylation of other core APC/C subunits, is required for the inhibition of APC/C^{Cdc20} by Bub1. However, it cannot be ruled out that phosphorylation of APC/C itself by Bub1 also contributes to APC/C inhibition.

The Kinase Activity of Bub1 toward Cdc20 Is Stimulated upon Checkpoint Activation

We next tested whether the kinase activity of Bub1 was enhanced in checkpoint-active cells. Bub1-Bub3 was immunoprecipitated from various HeLa cell lysates and incubated with recombinant Cdc20 in the presence of ^{32}P-ATP. Similar amounts of Bub1 were retained on the Bub1 antibody beads from the thymidine-, nocodazole-, and Taxol-arrested HeLa cell lysates (Figure 5C). Consistent with earlier reports (Taylor et al., 2001), the gel mobility of Bub1 from HeLa cells arrested with nocodazole and Taxol was slower than that of Bub1 from log phase or thymidine arrested HeLa cells (Figure 5C). Phosphatase treatment reversed this mobility shift of Bub1, suggesting that Bub1 was hyperphosphorylated in checkpoint-active cells (Figure 5C). Furthermore, the Bub1-Bub3 complexes isolated from nocodazole- or Taxol-arrested (metaphase) cells exhibited much higher kinase activity toward Cdc20 as compared to Bub1 immunoprecipitated from the thymidine-arrested (G1/S) cells (Figure 5D). The endogenous Bub1-Bub3 complex also phosphorylated Cdc20 at the same six sites described above, since Cdc20^{BPM} was not significantly phosphorylated by the Bub1 immunoprecipitates (IP)

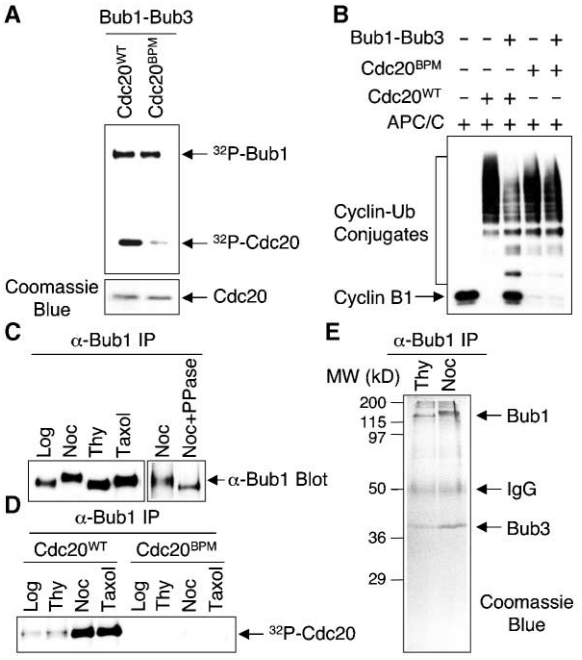

Figure 5. Generation of a Cdc20 Mutant Resistant to Bub1 Phosphorylation and Checkpoint Stimulation of the Kinase Activity of Bub1 toward Cdc20

(A) Recombinant Cdc20^{WT} and Cdc20^{BPM} proteins were incubated with Bub1-Bub3 in the presence of γ-^{32}P-ATP for 30 min at room temperature. All six serine/threonine residues of Cdc20 shown to be phosphorylated in vivo (Figure 4) were mutated to alanines in Cdc20^{BPM}. The reaction mixture was quenched with SDS sample buffer, separated on SDS-PAGE, and analyzed by autoradiography. The position of phosphorylated Cdc20 is indicated. The bottom panel shows a Coomassie-stained gel of the same reactions to indicate that equal amounts of Cdc20^{WT} and Cdc20^{BPM} were present in these reactions.

(B) APC/C was isolated from interphase *Xenopus* egg extracts and incubated with recombinant human Cdc20^{WT} or Cdc20^{BPM} proteins, in the presence of buffer or Bub1-Bub3 with the addition of ATP. The ubiquitination activity of APC/C was assayed with a Myc-tagged N-terminal fragment (residues 1–102) of human cyclin B1. The reaction mixtures were separated on SDS-PAGE and blotted with the anti-Myc antibody. The positions of the cyclin B1 substrate and the cyclin B1-ubiquitin conjugates are labeled.

(C) The endogenous Bub1 protein was immunoprecipitated from log phase, nocodazole-arrested, thymidine-arrested, and Taxol-arrested HeLa cell lysates, and blotted with anti-Bub1. In a separate experiment, the Bub1 IP from nocodazole-arrested cells was also treated with λ-phosphatase.

(D) Recombinant Cdc20^{WT} and Cdc20^{BPM} proteins were incubated with the Bub1 immunoprecipitates described in (C) in the presence of γ-^{32}P-ATP for 30 min at room temperature. The reaction mixture was quenched with SDS sample buffer, separated on SDS-PAGE, and analyzed by autoradiography. The position of phosphorylated Cdc20 is indicated.

(E) The endogenous Bub1 complex was immunoprecipitated from thymidine- or nocodazole-arrested HeLa cell lysates and separated by SDS-PAGE followed by Coomassie staining. The bands corresponding to Bub1 and Bub3 are indicated.

(Figure 5D). In addition, we performed a large-scale immunoprecipitation of the endogenous Bub1 complex. Based on Coomassie staining, Bub1 and Bub3 were the only stoichiometric components of the Bub1 complex in either thymidine- or nocodazole-treated HeLa cells (Figure 5E). Therefore, upon checkpoint activation, Bub1 is hyperphosphorylated and its kinase activity toward Cdc20 is stimulated. However, we cannot rule out the possibility that the Bub1 IPs contain substoichiometric amounts of other kinases.

Expression of the Nonphosphorylatable Cdc20 Mutant in HeLa Cells Causes Defects in the Spindle Checkpoint

To determine the in vivo consequence of Bub1-mediated Cdc20 phosphorylation, we established HeLa cell lines stably transfected with plasmids expressing either Myc-Cdc20^{WT} or Myc-Cdc20^{BPM} driven by a tetracycline-inducible promoter. The effects of induced expression of Myc-Cdc20^{WT} or Myc-Cdc20^{BPM} on the spindle checkpoint were assessed by the addition of nocodazole or Taxol to these cells. Because gross overexpression of the wild-type Cdc20 protein causes cells to escape from mitotic arrest in the presence of nocodazole, we chose cell lines that, when induced, expressed Myc-Cdc20 proteins at levels comparable to the endogenous Cdc20. We obtained multiple such clones of each stable cell line. There was little clonal variation in the following experiments (data not shown). A representative clone for each cell line was shown. In the absence of doxycycline, more than 90% of the Myc-Cdc20^{WT}-expressing cells arrested in mitosis in the presence of nocodazole or Taxol (Figures 6A and 6B). Induced expression of Myc-Cdc20^{WT} to a level 2- to 3-fold above the endogenous Cdc20 protein did not appreciably alter the mitotic index of these cells in the presence of spindle damage (Figures 6A, 6B, and 6D). Similar to Myc-Cdc20^{WT}-expressing cells, in the absence of doxycycline, about 80%–90% of the Myc-Cdc20^{BPM}-expressing cells arrested in the presence of nocodazole or Taxol. However, when the expression of Myc-Cdc20^{BPM} was induced by the addition of doxycycline, only 40%–50% of the Myc-Cdc20^{BPM}-expressing cells remained arrested in mitosis (Figures 6A, 6B, and 6D). Consistent with a partially defective spindle checkpoint in cells with induced expression of Myc-Cdc20^{BPM}, FACS analysis revealed that a fraction of these cells exited from mitosis in the absence of cytokinesis, resulting in the accumulation of interphase cells with 4N DNA contents (data not shown). After a prolonged exposure to nocodazole (48 hr), 31.2% of cells had undergone another round of DNA replication in the absence of cell division (Figure 6C), a hallmark of cells with a defective spindle checkpoint. In contrast, the majority of the Myc-Cdc20^{WT}-expressing cells remained arrested in mitosis with 4N DNA contents. Prolonged exposure to nocodazole caused a significant fraction of the cells to undergo cell death while only 5.3% of the cells possessed DNA contents greater than 4N (Figure 6C).

We also examined the protein levels of securin, the key APC/C^{Cdc20} substrate involved in this checkpoint. Addition of nocodazole or Taxol to Myc-Cdc20^{WT} or Myc-Cdc20^{BPM} cells led to the accumulation of securin (Figure 6D). Induced expression of Myc-Cdc20^{WT} did not alter the protein levels of securin. In contrast, the securin level was much lower in cells with an elevated expression of Myc-Cdc20^{BPM}, consistent with the fact that a significant percentage of the Myc-Cdc20^{BPM}-expressing cells escaped mitosis in the presence of spindle damage. Taken together, these data indicate that modest overexpres-

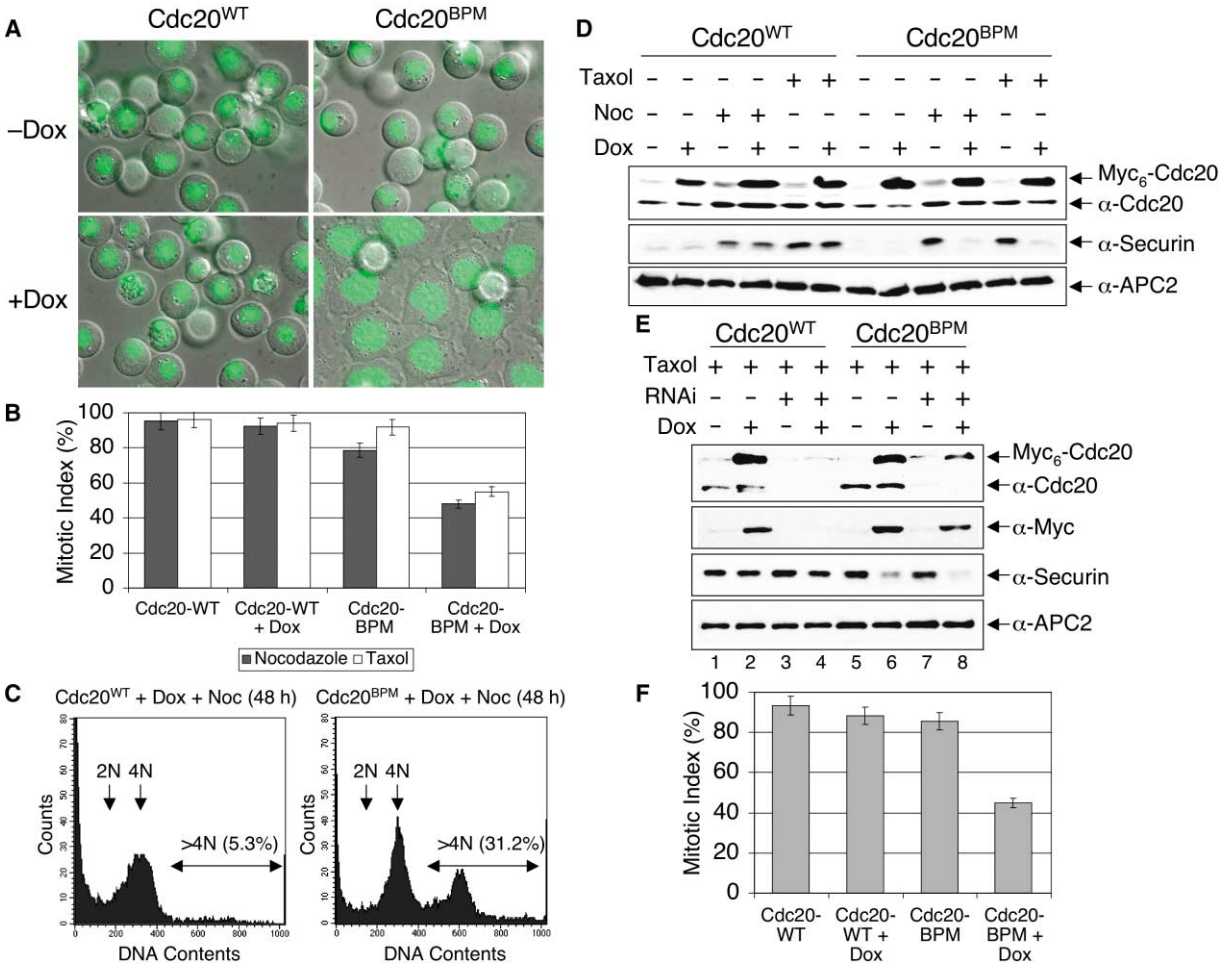

Figure 6. HeLa Cells Expressing Cdc20^{BPM} Are Partially Defective in the Spindle Checkpoint

(A) HeLa Tet-on cells stably transfected with Cdc20^{WT} or Cdc20^{BPM} were cultured in the absence or presence of doxycycline, treated with nocodazole for 16 hr, stained with Hoechst 33342, and directly visualized using an inverted fluorescence microscope. The DIC images are shown in gray and DNA is shown in green.

(B) HeLa Tet-on cells stably transfected with Cdc20^{WT} or Cdc20^{BPM} were cultured in the absence or presence of doxycycline, treated with nocodazole or Taxol for 16 hr, and directly visualized using an inverted fluorescence microscope. The mitotic index of these cells was measured by counting three fields of more than 100 cells.

(C) FACS analysis of Cdc20^{WT}- or Cdc20^{BPM}-expressing HeLa Tet-on cells cultured in the presence of doxycycline and treated with nocodazole for 48 hr. The 2N and 4N peaks are labeled. The percentage of cells with greater than 4N DNA contents is indicated.

(D) HeLa Tet-on cells stably transfected with Cdc20^{WT} or Cdc20^{BPM} were cultured in the absence or presence of doxycycline and treated with nocodazole or Taxol for 16 hr. The cells were dissolved in SDS sample buffer, separated on SDS-PAGE, and blotted with the indicated antibodies.

(E) HeLa Tet-on cells stably transfected with Cdc20^{WT} or Cdc20^{BPM} were cultured in the absence or presence of doxycycline and transfected with control or Cdc20 siRNA. 48 hours after siRNA transfection, the cells were treated with Taxol for 16 hr. The cells were then dissolved in SDS sample buffer, separated on SDS-PAGE, and blotted with the indicated antibodies.

(F) The mitotic index of the same cell samples described in (E).

sion of Cdc20^{BPM} compromises the integrity of the spindle checkpoint in the presence of spindle damage.

We tested whether Cdc20^{BPM} promoted mitotic exit in the absence of wild-type endogenous Cdc20 protein. To do so, we chose an siRNA oligonucleotide duplex in a region harboring one of the six mutations of Cdc20^{BPM}. This Cdc20 siRNA greatly reduced the expression of both the endogenous Cdc20 and Myc-Cdc20^{WT} proteins while it only slightly reduced the protein level of Myc-Cdc20^{BPM} (Figure 6E). At a level comparable to the endogenous Cdc20 protein (compare lanes 4 and 8 of Figure 6E), Myc-Cdc20^{BPM} caused a reduction of the protein level of securin and about 50% of the cells to escape from the mitotic arrest exerted by nocodazole (Figures 6E and 6F). Thus, elimination of Bub1 phosphorylation sites of Cdc20 causes a defect in the spindle checkpoint in HeLa cells. This further supports a functional role of Bub1-mediated phosphorylation of Cdc20 in vivo.

Recently, *Xenopus* Cdc20 has been shown to be phosphorylated on four serine/threonine residues during mitosis, and these phosphorylation events are required for the efficient binding between Cdc20 and spindle checkpoint proteins, such as BubR1 and Mad2 (Chung and Chen, 2003). Only one of the four corresponding residues (Ser41) was phosphorylated in hu-

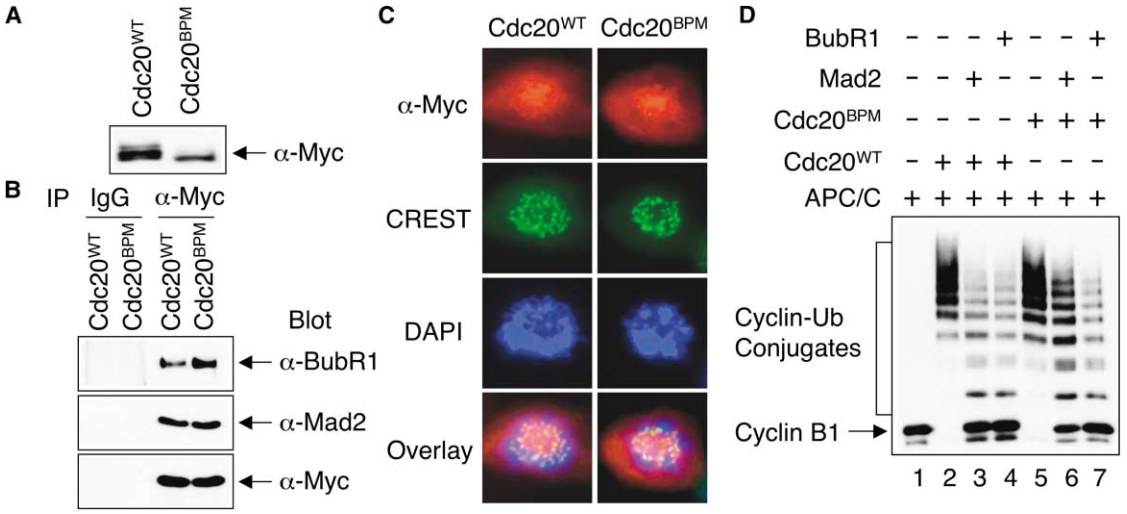

Figure 7. Cdc20^{BPM} Retains the Ability to Bind to BubR1 and Mad2

(A) HeLa Tet-on cells stably transfected with Cdc20^{WT} or Cdc20^{BPM} were cultured in the absence of doxycycline and treated with nocodazole for 16 hr. The mitotic cells were shaken off the plates, lysed, and immunoblotted with α-Myc.

(B) HeLa Tet-on cells stably transfected with Cdc20^{WT} or Cdc20^{BPM} were cultured in the presence of doxycycline and treated with nocodazole for 16 hr. The mitotic cells were shaken off the plates, lysed, and immunoprecipitated with either control IgG or α-Myc antibodies. The immunoprecipitates were blotted with the indicated antibodies.

(C) Mitotic HeLa cells expressing Cdc20^{WT} or Cdc20^{BPM} were fixed and stained with α-Myc (red), CREST (green), or DAPI (blue).

(D) APC/C was isolated from interphase *Xenopus* egg extracts and incubated with recombinant human Cdc20^{WT} or Cdc20^{BPM} proteins, in the presence of buffer, recombinant bacterially expressed Mad2 oligomer, or BubR1-Bub3 expressed in Sf9 cells. The ubiquitination activity of APC/C was assayed with a Myc-tagged N-terminal fragment (residues 1–102) of human cyclin B1. The reaction mixtures were separated on SDS-PAGE and blotted with the anti-Myc antibody. The positions of the cyclin B1 substrate and the cyclin B1-ubiquitin conjugates are labeled.

man Cdc20. To confirm that the six phosphorylation sites of Cdc20 identified by mass spectrometry in this study are relevant, we compared the phosphorylation patterns of Myc-Cdc20^{WT} and Myc-Cdc20^{BPM} in mitosis. Similar to the endogenous Cdc20 protein, a significant fraction of Myc-Cdc20^{WT} underwent gel mobility shift in mitosis (Figure 7A). In contrast, Myc-Cdc20^{BPM} lacked these slower migrating forms of Cdc20, indicating that at least a subset of these sites of Cdc20 were phosphorylated in vivo (Figure 7A).

We next checked whether Cdc20^{BPM} interacted with BubR1 and Mad2. After treatment with doxycycline, mitotic Myc-Cdc20^{WT} and Myc-Cdc20^{BPM}-expressing cells were collected with mitotic shake-off. The lysates of these cells were then immunoprecipitated with anti-Myc antibody beads and blotted with anti-BubR1 and anti-Mad2 antibodies. Similar amounts of BubR1 and Mad2 were present in the Cdc20^{WT} and Cdc20^{BPM} immunoprecipitates (Figure 7B), indicating that Cdc20^{BPM} still retained the ability to bind to BubR1 and Mad2. We also examined the cellular localization of Cdc20^{BPM}. Both Cdc20^{WT} and Cdc20^{BPM} localized to kinetochores during mitosis (Figure 7C). Finally, Cdc20^{BPM} was efficiently inhibited by either Mad2 or BubR1 in the APC/C ubiquitination assay (Figure 7D). Therefore, phosphorylation of Cdc20 at these six sites is not required for Mad2 and BubR1 binding to Cdc20. The fact that Cdc20^{BPM} is still inhibited by Mad2 and BubR1 might also explain why Cdc20^{BPM}-expressing cells are only partially defective in the spindle checkpoint.

Discussion

Genetic and biochemical studies have implicated Bub1 as an upstream component of the spindle checkpoint pathway. The data presented herein revealed a surprisingly direct role of Bub1 in blocking the activity of APC/C^{Cdc20}, a molecular target of the checkpoint.

Role of Bub1-Mediated Cdc20 Phosphorylation in the Spindle Checkpoint

There is some controversy with respect to the requirement of the kinase activity of Bub1 in the spindle checkpoint. First, budding yeast cells harboring a kinase-inactive mutant of Bub1 (Bub1^{K733R}) exhibit a defective spindle checkpoint, indicating a requirement for the kinase activity of Bub1 in checkpoint signaling (Roberts et al., 1994). Likewise, the kinase activity of Bub1 is required for the intactness of the spindle checkpoint in fission yeast (Yamaguchi et al., 2003). On the other hand, addition of a kinase-inactive mutant of Bub1 to *Xenopus* egg extracts depleted for the endogenous Bub1 protein restores the spindle checkpoint, suggesting that the kinase activity of Bub1 is not essential for checkpoint signaling in *Xenopus* egg extracts (Sharp-Baker and Chen, 2001). However, the kinase activity of Bub1 is required for the checkpoint under low concentrations of nuclei or nocodazole (Chen, 2004). In budding yeast, an N-terminal fragment of Bub1 lacking the kinase domain is sufficient for checkpoint signaling in the presence of spindle-damaging agents (Warren et al., 2002). However, a C-terminal fragment of Bub1 containing the kinase domain has been shown to contribute to the fidelity of chromosome segregation (Warren et al., 2002). At present, it is unclear whether these discrepancies on the role of the Bub1 kinase activity reflect genuine differences in the signaling mechanisms of the spindle checkpoint in various organisms or whether they are caused by limitations in certain experimental systems.

We have so far failed to establish mammalian cell lines stably expressing either the wild-type or the kinase-inactive mutant of Bub1 to a level comparable to that of the endogenous Bub1 protein. This precludes us from examining whether a kinase-inactive mutant of Bub1 can rescue the checkpoint defect in mammalian cells depleted for Bub1 by RNAi. However, Bub1 is a key molecular component of the spindle checkpoint in various organisms. Its kinase domain is strictly conserved during evolution. It would be surprising if the kinase activity of Bub1 were not required for its major biological function. The data presented herein support a role for the Bub1 kinase activity in the spindle checkpoint.

There are also conflicting reports about the role of Cdc20 phosphorylation in the regulation of the APC/C activity. Phosphorylation of Cdc20 by Cdk1 has been reported to activate APC/C (Kotani et al., 1999). In contrast, Yudkovsky et al. have shown that phosphorylation of Cdc20 by Cdk1 inhibited APC/C^{Cdc20} (Yudkovsky et al., 2000). Yet another study claims that phosphorylation of Cdc20 has no effect on the activity of APC/C (Kramer et al., 2000). Very recently, it has been suggested that an active Cdk1 is required for the spindle checkpoint, and phosphorylation of Cdc20 by Cdk1 prevents its binding to APC/C (D'Angiolella et al., 2003). However, these studies did not fully determine the actual sites of phosphorylation on Cdc20. It is conceivable that phosphorylation of Cdc20 at different sites might have different functional consequences. We have now mapped the phosphorylation sites on Cdc20 by Bub1 and showed that phosphorylation of these six sites or a subset of these sites on Cdc20 by Bub1 inhibits the activity of APC/C. Elimination of these sites within Cdc20 renders it refractory to Bub1 phosphorylation and inhibition in vitro, and causes a defective spindle checkpoint in vivo. In addition, the Bub1 kinase activity toward Cdc20 is stimulated in cells with an activated spindle checkpoint. These results argue strongly that phosphorylation of Cdc20 by Bub1 is required for proper spindle checkpoint signaling.

Multiple Mechanisms for the Inhibition of APC/C^{Cdc20} by Checkpoint Proteins

Previous studies have established that Mad2 and BubR1 (the vertebrate homolog of Mad3) act synergistically to inhibit APC/C^{Cdc20} in vitro even though each of them alone is capable of inhibiting APC/C (Tang et al., 2001; Fang, 2002). BubR1 and Mad2 might function in a single mitotic checkpoint complex (MCC) containing BubR1, Bub3, Cdc20, and Mad2 (Sudakin et al., 2001; Chen, 2002). These APC/C inhibitors inhibit APC/C through stoichiometric binding to Cdc20. In contrast, a substoichiometric amount of Bub1 efficiently inhibits APC/C^{Cdc20} in vitro. This inhibition requires the kinase activity of Bub1. These findings indicate that Bub1 inhibits APC/C^{Cdc20} in a catalytic fashion. Furthermore, we have shown that Bub1-mediated phosphorylation of Cdc20 is not required for its binding to BubR1 or Mad2. Yet, expression of a Cdc20 mutant resistant to Bub1 phosphorylation results in a partially defective spindle checkpoint in living cells. This suggests that phosphorylation of Cdc20 by Bub1 is an important APC/C-inhibitory mechanism of the spindle checkpoint. In the future, it will be important to determine how and to what extent these multiple APC/C inhibitory mechanisms contribute to spindle checkpoint signaling during the normal cell cycle and under different spindle damaging conditions.

In conclusion, we have uncovered an unexpected role of Bub1 in the spindle checkpoint. An important and yet largely unexplained feature of the spindle checkpoint is that a single unattached kinetochore can delay the onset of sister-chromatid separation (Rieder et al., 1995). It has been postulated that this kinetochore generates diffusible "wait anaphase" signals to inhibit APC/C^{Cdc20} (Shah and Cleveland, 2000; Yu, 2002). Mad2 turns over rapidly at the unattached kinetochores, and thus Mad2-containing checkpoint complexes are likely to be a part of the diffusible checkpoint signals (Howell et al., 2000; Shah and Cleveland, 2000). However, these checkpoint complexes inhibit APC/C through direct stoichiometric binding. In contrast, Bub1 inhibits APC/C^{Cdc20} catalytically and its kinase activity toward Cdc20 is stimulated upon checkpoint activation, suggesting a direct involvement of Bub1 in the elusive diffusible signals.

Experimental Procedures

Antibodies, Immunoblotting, and Immunoprecipitation

To generate antibodies against Bub3 and Cdc20, the full-length Bub3 protein with an N-terminal His_6 tag was expressed in Sf9 insect cells and purified with Ni^{2+}-NTA beads. The N-terminal domain of Cdc20 (residues 1–174) was produced in bacteria as an N-terminal GST-fusion protein and purified using glutathione agarose beads. The purified proteins were used to immunize rabbits at Zymed Laboratories (San Francisco, CA). The antisera were purified using the appropriate antigens. The production of the Bub1, BubR1, Mad2, and APC2 antibodies was described previously (Fang et al., 1998b; Tang et al., 2001). The cyclin B1 antibody was purchased from Santa Cruz Biotechnology. For immunoblotting, the antibodies were used at 1:1000 dilution of crude sera or at 1 μg/ml of affinity-purified IgG.

For immunoprecipitation, affinity-purified antibodies against Bub1 and Cdc20 were coupled to Affi-Prep Protein A beads (Bio-Rad) at a concentration of 1 mg/ml. HeLa cells at various cell cycle stages were lysed with the NP-40 lysis buffer (50 mM Tris-HCl [pH 7.7], 150 mM NaCl, 0.5% NP-40, 1 mM DTT, 10% glycerol, 0.5 μM okadaic acid, and 10 μg/ml each of leupeptin, pepstatin, and chymostatin). For immunoprecipitation of Bub1, the lysates were cleared by centrifuging for 30 min at 4°C at top speed in a microcentrifuge to make the high-speed supernatants. The antibody beads were incubated with the HeLa cell supernatants for 2 hr at 4°C. The beads were then washed five times with the NP-40 lysis buffer. The proteins bound to the beads were either used directly in kinase assays (see below) or dissolved in SDS sample buffer, separated by SDS-PAGE, and blotted with the desired antibodies. The large-scale immunopurification of Cdc20 was performed essentially as described above with the following modifications. HeLa cell lysates were cleared by centrifuging at 100,000 × g for 1 hr at 4°C. The Cdc20 protein bound to antibody beads was eluted with 100 mM glycine (pH 2.5), concentrated with a microcon (Millipore), separated on SDS-PAGE, and stained with colloidal Coomassie blue (Pierce).

Tissue Culture and Transfection

HeLa Tet-on (Clontech) or HeLa S3 cells were grown in Dulbecco's modified Eagle's medium (DMEM; Invitrogen) supplemented with 10% fetal bovine serum, 2 mM L-glutamine, 100 μg/ml penicillin, and streptomycin. To arrest cells at G1/S, cells were grown in the presence of 2 mM thymidine (Sigma) for 18 hr. To block cells in mitosis, cells were treated with 300 nM nocodazole (Sigma) or 100 nM Taxol (Calbiochem) for 18 hr. To release the nocodazole-mediated mitotic arrest, HeLa cells were washed twice with fresh medium and replated. Samples were taken at the indicated time points and processed for immunoblotting and FACS.

To establish Myc-$Cdc20^{WT}$- and Myc-$Cdc20^{BPM}$-expressing stable cell lines, HeLa Tet-on cells at 40%–50% confluency were transfected with the pTRE2-Myc-$Cdc20^{WT}$ or pTRE2-Myc-$Cdc20^{BPM}$ plas-

mids using the Effectene reagent (Qiagen) according to manufacturer's protocol. The transfected cells were then selected with 300 μg/ml of hygromycin (Clontech). The surviving clones were expanded and screened for the induced expression of Myc-Cdc20^{WT} or Myc-Cdc20^{BPM} in the absence and presence of 300 μg/ml doxycycline (Clontech).

The siRNA oligonucleotides targeting Bub1 and Cdc20 were chemically synthesized at Dharmacon or at an in-house facility, and contained sequences corresponding to nucleotides 382–404 (Bub1 siRNAa) and nucleotides 273–295 (Bub1 siRNAb) of the Bub1 coding region and nucleotides 198–220 of human Cdc20. The annealing of the siRNAs and subsequent transfection of the RNA duplexes into HeLa Tet-on cells were performed using the Oligofectamine reagent (Invitrogen) exactly as described (Elbashir et al., 2001).

Identification of Phosphorylation Sites by Tandem Mass Spectrometry

Phosphorylation sites of Cdc20 were identified by a combination of precursor ion scanning and nanoelectrospray tandem mass spectrometry (MS/MS). Briefly, the colloidal blue-stained Cdc20 protein bands were excised from 1D SDS-PAGE gels and subjected to in-gel digestion with trypsin. The dried protein digests were dissolved in 5% formic acid and loaded onto a pulled capillary filled with POROS R2 resin. After washing three times with 5% formic acid, the peptides were eluted into a nanoelectrospray needle with 1–2 μl of nanoelectrospray sample solution for either precursor ion scanning in negative ion mode, or MS/MS in positive ion mode. All mass spectrometry (MS) analyses were performed on a QSTAR Pulsar-i quadrupole time-of-flight tandem mass spectrometer (Applied Biosystems/MDS Sciex, Toronto, ON, Canada) equipped with a nanoelectrospray ion source (MDS Proteomics, Odense, Denmark). For precursor ion scanning experiments, the instrument was set in negative ion mode, with the quadrupole Q2 pulsing function turned on, to detect the PO^{3-} fragment ion at m/z −79. The optimum collision energies were determined for each experiment by gradually increasing the voltage of Q0 in steps corresponding to one-twentieth of the m/z value of the precursor ion. After data acquisition by precursor ion scanning, the instrument was switched to positive ion mode, and the phosphopeptide sequence and sites of phosphorylation were identified by nanoelectrospray Tandem mass spectrometry (MS/MS). In the MS/MS scan mode, precursor ions were selected in quadrupole Q1 and fragmented in the collision cell (q2), using argon as the collision gas.

Microscopy and Flow Cytometry

HeLa-H2B-GFP cells were transfected with the control and Bub1 siRNA duplexes. After 36 hr, cells were treated with 300 nM nocodazole for 16 hr and directly observed with a Zeiss Axiovert 200M inverted fluorescence microscope using a 40× objective. In the case of Cdc20^{WT}- and Cdc20^{BPM}-expressing cells, these cells were grown in the absence or presence of doxycycline and treated with nocodazole or Taxol. The cells were stained with Hoeschst 33342 and directly observed with a Zeiss Axiovert 200M inverted fluorescence microscope using a 63× objective. Alternatively, cells were fixed by 70% ethanol, stained with propidium iodide, and analyzed by flow cytometry (FACS).

For immunostaining, HeLa Tet-on cells expressing Myc-Cdc20^{WT} or Myc-Cdc20^{BPM} were grown to 50%–70% confluency in the presence of doxycycline, fixed with 4% paraformaldehyde, permeablized with 0.1% Triton-X100 in PBS, and incubated with 1 μg/ml of anti-Myc antibody. The cells were also stained with 1:2000 dilution of a human CREST autoimmune serum. After washing, fluorescent secondary antibodies against mouse or human IgGs were added at 1:500 dilutions. The cells were again washed three times in PBS, and viewed using a 63× objective on a Zeiss Axiovert 200M inverted fluorescence microscope.

Kinase and Ubiquitination Assays

The expression and purification of human Bub1, Bub1^{K821A}, Bub3, Cdc20, Cdc20^{BPM}, and Cdh1 proteins in Sf9 cells were described previously (Tang and Yu, 2004). The kinase assays were performed in 30 μl reactions. Each reaction contained 100 nM Bub1-Bub3, 1 μM Cdc20, 30 μM cold ATP, and 8 μCi ^{32}P-ATP in KB buffer (50 mM Tris-HCl [pH 7.7], 100 mM KCl, 10 mM $MgCl_2$, 1 mM DTT). For the IP kinase assays, the Bub1 immunoprecipitates were obtained as described above and used in the kinase reactions instead of the recombinant kinases. The reactions were incubated at room temperature for 30 min, quenched with SDS sample buffer, and analyzed by SDS-PAGE followed by autoradiography. The in vitro APC/C ubiquitination assay was performed as described (Tang and Yu, 2004).

Acknowledgments

We thank Bing Li for the affinity purification of the Bub3 antibody, Guohong Xia for making the Cdc20 baculovirus, and Bing-e Xu and Melanie Cobb for providing p38MAPK and ERK1 proteins. We also thank Rey-Huei Chen, Orna Cohen-Fix, Andy Hoyt, Xuelian Luo, Frank McKeon, Hui Zou, and members of the Yu laboratory for helpful discussions and for reading the manuscript critically. H.Y. is the Michael L. Rosenberg Scholar in Biomedical Research. This work is supported by the National Institutes of Health (GM61542), the Packard Foundation, the W.M. Keck Foundation, the March of Dimes Foundation, and the Leukemia and Lyophoma Society.

Received: December 20, 2003
Revised: July 30, 2004
Accepted: August 24, 2004
Published: November 4, 2004

References

Bharadwaj, R., and Yu, H. (2004). The spindle checkpoint, aneuploidy, and cancer. Oncogene *23*, 2016–2027.

Brady, D.M., and Hardwick, K.G. (2000). Complex formation between Mad1p, Bub1p and Bub3p is crucial for spindle checkpoint function. Curr. Biol. *10*, 675–678.

Chen, R.H. (2002). BubR1 is essential for kinetochore localization of other spindle checkpoint proteins and its phosphorylation requires Mad1. J. Cell Biol. *158*, 487–496.

Chen, R.H. (2004). Phosphorylation and activation of Bub1 on unattached chromosomes facilitate the spindle checkpoint. EMBO J. *23*, 3113–3121.

Chung, E., and Chen, R.H. (2003). Phosphorylation of Cdc20 is required for its inhibition by the spindle checkpoint. Nat. Cell Biol. *5*, 748–753.

D'Angiolella, V., Mari, C., Nocera, D., Rametti, L., and Grieco, D. (2003). The spindle checkpoint requires cyclin-dependent kinase activity. Genes Dev. *17*, 2520–2525.

Elbashir, S.M., Harborth, J., Lendeckel, W., Yalcin, A., Weber, K., and Tuschl, T. (2001). Duplexes of 21-nucleotide RNAs mediate RNA interference in cultured mammalian cells. Nature *411*, 494–498.

Fang, G. (2002). Checkpoint protein BubR1 acts synergistically with Mad2 to inhibit anaphase-promoting complex. Mol. Biol. Cell *13*, 755–766.

Fang, G., Yu, H., and Kirschner, M.W. (1998a). The checkpoint protein MAD2 and the mitotic regulator CDC20 form a ternary complex with the anaphase-promoting complex to control anaphase initiation. Genes Dev. *12*, 1871–1883.

Fang, G., Yu, H., and Kirschner, M.W. (1998b). Direct binding of CDC20 protein family members activates the anaphase-promoting complex in mitosis and G1. Mol. Cell *2*, 163–171.

Farr, K.A., and Hoyt, M.A. (1998). Bub1p kinase activates the Saccharomyces cerevisiae spindle assembly checkpoint. Mol. Cell. Biol. *18*, 2738–2747.

Harper, J.W., Burton, J.L., and Solomon, M.J. (2002). The anaphase-promoting complex: it's not just for mitosis any more. Genes Dev. *16*, 2179–2206.

Howell, B.J., Hoffman, D.B., Fang, G., Murray, A.W., and Salmon, E.D. (2000). Visualization of Mad2 dynamics at kinetochores, along spindle fibers, and at spindle poles in living cells. J. Cell Biol. *150*, 1233–1250.

Kotani, S., Tanaka, H., Yasuda, H., and Todokoro, K. (1999). Regula-

tion of APC activity by phosphorylation and regulatory factors. J. Cell Biol. *146*, 791–800.

Kraft, C., Herzog, F., Gieffers, C., Mechtler, K., Hagting, A., Pines, J., and Peters, J.M. (2003). Mitotic regulation of the human anaphase-promoting complex by phosphorylation. EMBO J. *22*, 6598–6609.

Kramer, E.R., Scheuringer, N., Podtelejnikov, A.V., Mann, M., and Peters, J.M. (2000). Mitotic regulation of the APC activator proteins CDC20 and CDH1. Mol. Biol. Cell *11*, 1555–1569.

Luo, X., Fang, G., Coldiron, M., Lin, Y., Yu, H., Kirschner, M.W., and Wagner, G. (2000). Structure of the Mad2 spindle assembly checkpoint protein and its interaction with Cdc20. Nat. Struct. Biol. *7*, 224–229.

Luo, X., Tang, Z., Rizo, J., and Yu, H. (2002). The Mad2 spindle checkpoint protein undergoes similar major conformational changes upon binding to either Mad1 or Cdc20. Mol. Cell *9*, 59–71.

Luo, X., Tang, Z., Xia, G., Wassmann, K., Matsumoto, T., Rizo, J., and Yu, H. (2004). The Mad2 spindle checkpoint protein has two distinct natively folded states. Nat. Struct. Mol. Biol. *11*, 338–345.

Musacchio, A., and Hardwick, K.G. (2002). The spindle checkpoint: structural insights into dynamic signalling. Nat. Rev. Mol. Cell Biol. *3*, 731–741.

Nasmyth, K. (2002). Segregating sister genomes: the molecular biology of chromosome separation. Science *297*, 559–565.

Nasmyth, K., Peters, J.M., and Uhlmann, F. (2000). Splitting the chromosome: cutting the ties that bind sister chromatids. Science *288*, 1379–1385.

Nicklas, R.B. (1997). How cells get the right chromosomes. Science *275*, 632–637.

Peters, J.M. (2002). The anaphase-promoting complex. Proteolysis in mitosis and beyond. Mol. Cell *9*, 931–943.

Rieder, C.L., Cole, R.W., Khodjakov, A., and Sluder, G. (1995). The checkpoint delaying anaphase in response to chromosome mono-orientation is mediated by an inhibitory signal produced by unattached kinetochores. J. Cell Biol. *130*, 941–948.

Roberts, B.T., Farr, K.A., and Hoyt, M.A. (1994). The Saccharomyces cerevisiae checkpoint gene BUB1 encodes a novel protein kinase. Mol. Cell. Biol. *14*, 8282–8291.

Seeley, T.W., Wang, L., and Zhen, J.Y. (1999). Phosphorylation of human MAD1 by the BUB1 kinase in vitro. Biochem. Biophys. Res. Commun. *257*, 589–595.

Shah, J.V., and Cleveland, D.W. (2000). Waiting for anaphase: Mad2 and the spindle assembly checkpoint. Cell *103*, 997–1000.

Sharp-Baker, H., and Chen, R.H. (2001). Spindle checkpoint protein Bub1 is required for kinetochore localization of Mad1, Mad2, Bub3, and CENP-E, independently of its kinase activity. J. Cell Biol. *153*, 1239–1250.

Sironi, L., Mapelli, M., Knapp, S., Antoni, A.D., Jeang, K.T., and Musacchio, A. (2002). Crystal structure of the tetrameric Mad1-Mad2 core complex: implications of a "safety belt" binding mechanism for the spindle checkpoint. EMBO J. *21*, 2496–2506.

Sudakin, V., Chan, G.K., and Yen, T.J. (2001). Checkpoint inhibition of the APC/C in HeLa cells is mediated by a complex of BUBR1, BUB3, CDC20, and MAD2. J. Cell Biol. *154*, 925–936.

Tang, Z., and Yu, H. (2004). Functional analysis of the spindle-checkpoint proteins using an in vitro ubiquitination assay. Methods Mol. Biol. *281*, 227–242.

Tang, Z., Bharadwaj, R., Li, B., and Yu, H. (2001). Mad2-independent inhibition of APC^{Cdc20} by the mitotic checkpoint protein BubR1. Dev. Cell *1*, 227–237.

Taylor, S.S., Hussein, D., Wang, Y., Elderkin, S., and Morrow, C.J. (2001). Kinetochore localisation and phosphorylation of the mitotic checkpoint components Bub1 and BubR1 are differentially regulated by spindle events in human cells. J. Cell Sci. *114*, 4385–4395.

Warren, C.D., Brady, D.M., Johnston, R.C., Hanna, J.S., Hardwick, K.G., and Spencer, F.A. (2002). Distinct chromosome segregation roles for spindle checkpoint proteins. Mol. Biol. Cell *13*, 3029–3041.

Yamaguchi, S., Decottignies, A., and Nurse, P. (2003). Function of Cdc2p-dependent Bub1p phosphorylation and Bub1p kinase activity in the mitotic and meiotic spindle checkpoint. EMBO J. *22*, 1075–1087.

Yu, H. (2002). Regulation of APC-Cdc20 by the spindle checkpoint. Curr. Opin. Cell Biol. *14*, 706–714.

Yudkovsky, Y., Shteinberg, M., Listovsky, T., Brandeis, M., and Hershko, A. (2000). Phosphorylation of Cdc20/fizzy negatively regulates the mammalian cyclosome/APC in the mitotic checkpoint. Biochem. Biophys. Res. Commun. *271*, 299–304.